In silico directed chemical probing of the adenosine receptor family

Filipe M. Areias [a,b], Jose Brea [b], Elisabet Gregori-Puigjané [c], Magdi E. A. Zaki [a], M. Alice Carvalho [a], Eduardo Domínguez [b], Hugo Gutiérrez-de-Terán [b], M. Fernanda Proença [a], María I. Loza [b], Jordi Mestres [c,*]

[a] Center of Chemistry, Campus de Gualtar, Universidade do Minho, 4710-057 Braga, Portugal
[b] Department of Pharmacology, Universidade de Santiago de Compostela, 15782 Santiago de Compostela, Spain
[c] Chemotargets SL and Chemogenomics Laboratory, Research Unit on Biomedical Informatics, Institut Municipal d'Investigació Mèdica and Universitat Pompeu Fabra, 08003 Barcelona, Catalonia, Spain

ARTICLE INFO

ABSTRACT

One of the grand challenges in chemical biology is identifying a small-molecule modulator for each individual function of all human proteins. Instead of targeting one protein at a time, an efficient approach to address this challenge is to target entire protein families by taking advantage of the relatively high levels of chemical promiscuity observed within certain boundaries of sequence phylogeny. We recently developed a computational approach to identifying the potential protein targets of compounds based on their similarity to known bioactive molecules for almost 700 targets. Here, we describe the direct identification of novel antagonists for all four adenosine receptor subtypes by applying our virtual profiling approach to a unique synthesis-driven chemical collection composed of 482 biologically-orphan molecules. These results illustrate the potential role of in silico target profiling to guide efficiently screening campaigns directed to discover new chemical probes for all members of a protein family.

1. Introduction

The identification of the complete list of proteins to which small molecules could potentially have affinity is a cornerstone in the use of chemistry to probe biology, with important implications for modern drug discovery.[1] The compilation of large compound collections and the implementation of high-throughput screening, in both industry and academia, have increased dramatically our capacity to probe the chemical space for a single target. However, our capacity to probe the biological space of a single molecule is still limited, mainly due to the huge logistics involved in the systematic screening of molecules on a large panel of in vitro assays which, until recently, made these activities feasible only within the privacy of biotechnology and pharmaceutical industry.[2–4] In this respect, the launch of global coordinated initiatives, such as the NIH Molecular Libraries Screening Center Network (MLSCN)[5] and the Psychoactive Drug Screening Program (PDSP),[6] opens an avenue towards the consistent generation of screening data for molecules and the ultimate deposition of all chemical and biological data in public databases. In parallel, several informatics initiatives, such as DrugBank,[7] IUPHAR-DB,[8] and BindingDB[9] are complementing these experimental screening programs by collecting all pharmacological data being published in multiple bibliographical sources and making them accessible also in the public domain. Additionally, a growing number of entries containing a ligand forming a complex inside a protein cavity are being deposited in the Protein Data Bank,[10] the major public repository for protein structure information.

The availability of an increasing amount of protein–ligand interaction data has promoted the development of a variety of computational methods aiming at predicting the pharmacological profile of compounds,[11–13] and thus offering a perfect means to expand in silico our capacity to probe the biological space of molecules. Depending on the source of information being exploited, target profiling methods can be divided into ligand-based and structure-based methods: ligand-based methods rely essentially on comparing a target compound to a database of hundreds of thousands of chemical structures with known targets, whereas structure-based methods require three-dimensional information of the protein binding cavity to dock compounds in or assess their fitness relative to the exposed pharmacophoric features. Ligand-based target profiling methods were successfully applied recently to several drugs to detect additional proteins other than their recognized primary targets[14] and to predict the mechanism of action of antimalarials discovered in a high-throughput cell-based screen.[15] Likewise, structure-based target profiling methods allowed also for identifying a true target for some compounds in a scaffold-focused library[16] and to discover three targets associated with constituents of a medicinal plant.[17]

Here, we report the application of our own implementation of a ligand-based approach to in silico pharmacological profiling[18] to

identify the potential biological targets of a synthesis-driven compound collection and its subsequent use to complete the chemical probing of an entire protein family.

2. Results and discussion

2.1. Composition of the chemical library

Chemistry plays a fundamental role in our quest to probe and understand the biology of proteins and thus access to novel structural cores covering unexplored areas of chemical space is of utmost importance. Accordingly, our source of chemical matter was a unique collection composed of 482 biologically-orphan molecules synthesized and stored over the last few years at the Centre of Chemistry of the Universidade do Minho. The structural features of those molecules contained mainly aromatic heterocycles decorated with phenolic substituents obtained from commercially available starting materials, usually in multi-step processes, using a synthetic approach based primarily on methods developed internally for the synthesis of highly functionalised nitrogen heterocycles, which are difficult and costly to obtain otherwise. The exclusivity of the collection is reflected by the fact that only 11 of those 482 molecules were found available in the catalogues of chemical providers. The main core structures of this collection are compiled in Table 1. Substituted purines, including 8-oxopurines and imidazo-pyridines (S1, S2 and S3), correspond to approximately 43% of the compounds in the collection. Substituted imidazoles, 2-oxoimidazoles, imidazolyl-imidazolones and imidazo-imidazoles (S4, S5, S6 and S7) correspond to 24%. Pyrimido-pyrimidines and pyrido-pyrimidines (S8, S9 and S10) were generated by an ANRORC type rearrangement from some of the purine and imidazo-pyridine structures and correspond to 10%. A number of diaminomaleonitrile derivatives (S11) were also prepared, some of them were used as linear synthetic precursors of the cyclic compounds used in this study, and represent an additional 8% of the collection. The remaining 15% contain a diverse range of nitrogen heterocycles, including fused tricyclic structures.

2.2. In silico identification of putative targets

Given its structural composition, we decided to start profiling in silico the compound collection against a panel of 86 diverse G protein-coupled receptors (GPCRs) for which ligand-based models were available. Of the 482 molecules processed, only 23 received an annotation to at least one GPCR target. In total, 37 annotations were assigned to nine targets (Supplementary Table 1). Remarkably, all four adenosine receptors were included in the target hit list, collectively gathering 15 of those annotations from 10 different compounds. We saw in this outcome an opportunity to attempt for the first time the identification of novel hits for all members of a protein family by means of in silico profiling. Focus on adenosine receptors was also justified by the fact that they constitute a family of utmost biological importance and broad therapeutic relevance in cardiovascular, inflammatory, immune, and neurodegenerative diseases.[19,20] In addition, many of the adenosine receptor leads reported to date are xanthine or xanthine-like derivatives,[21] a core structure known to have issues with solubility and poor overall drug-like profile. Therefore, the discovery of novel chemical scaffolds in potent and selective bioactive compounds for adenosine receptors remains critical for a wide range of therapeutic areas.

2.3. In vitro screening against adenosine receptors

Complete in vitro screening of the 10 molecules against all four adenosine receptors was carried out at 10 µM concentration for competitive binding of specific radioligands to human A_1, A_{2A}, A_{2B}, and A_3 subtypes transfected cell lines (Table 2). Screening data confirmed the existence of two hits with specific binding displacements greater than 50% at the A_{2B} and A_3 adenosine receptors. These results allow for getting a fair assessment of the overall performance of the predictions made by in silico profiling. In this respect, it can be observed that not all compound–receptor interactions predicted to be active could be confirmed (2/15) and likewise not all inactive interactions were correctly anticipated (25/38). However, it is worth stressing that all 25 interactions predicted to be inactive were ultimately confirmed and, most importantly, the receptor affinities for the two hits identified were correctly predicted.

The structures of the two hits obtained from the primary screen for the A_{2B} and A_3 receptors are presented in Figure 1a. An analysis of these chemotypes against all bioactive compounds for the adenosine receptors present in the annotated chemical libraries used in this work confirmed the structural novelty of the hits. For the sake of clarity, the compounds will be referred to henceforth as MSB-A2B and MSB-A3. Further confirmation of the affinity and functional activity of the two compounds for their respective receptors is also included in Figure 1. Concentration-response binding competition curves revealed that both compounds had affinity values around the micromolar range, MSB-A2b and MSB-A3 showing pK_i values of 5.8 ± 0.3 and 6.5 ± 0.1 at the A_{2B} and A_3 receptors, respectively (Fig. 1b). Furthermore, the agonist/antagonist behaviour of these compounds was examined by measuring their modulation of NECA-dependent intracellular cAMP formation, which confirmed that the two compounds are antagonists of the A_{2B} and A_3 receptors with pK_b values of 5.7 ± 0.1 and 6.3 ± 0.4 for MSB-A2b and MSB-A3, respectively (Fig. 1c).

2.4. Complete probing of the adenosine receptor family

At this stage, our aim of chemically probing the entire adenosine receptor family had partially failed, since the primary screen of the compounds selected from our chemical collection did not deliver hits on the A_1 and A_{2A} receptors. Therefore, given the structural novelty of the hits identified for the A_{2B} and A_3 receptors, we decided to proceed by taking those structures as templates for a similarity-based virtual screening of the chemical catalogue composed of 7.5 million compounds available from commercial vendors using a set of low-dimensional descriptors that reflect the overall distribution of pharmacophoric features in a molecule (Supplementary Fig. 1).[22] A total of 9622 compounds were retrieved within a similarity cut-off of any of the two hits. In order to reduce the numbers further, those compounds were then profiled in silico against all four adenosine receptors and, to maximize the chances of identifying hits, those that could not be annotated to both A_1 and A_{2A} receptors were filtered out. The remaining 283 compounds were visually inspected and a set of eight compounds was finally agreed to be selected for purchase and testing based on their arrangement of the main pharmacophore features relative to those present in the most similar bioactive compounds to A_1 and A_{2A}. Complete in vitro screening of the eight molecules against the A_1 and A_{2A} receptors was carried out at the same conditions as described earlier. Screening data ultimately confirmed the existence of five hits with specific binding displacements greater than 50% at the A_1 and/or A_{2A} receptors (Table 3).

In agreement with the predicted in silico target profiling, three of the hits showed binding displacements greater than 50% for both A_1 and A_{2A} receptors, but most interestingly some degree of selectivity for A_1 and A_{2A}, respectively, was unexpectedly observed for the other two hits (Table 3). The structures of the two most selective hits obtained from the primary screen for the A_1 and A_{2A} receptors are presented in Figure 2a, which will be referred henceforth as MSB-A1 and MSB-A2a. Once more, an analysis of

Table 1
Main core structures and substitution patterns of the chemical library processed by in silico target profiling

Label	Core structure	Substitution pattern
S1		R = alkyl, aryl (including hydroxyphenyl) R^1 = H, aryl R^2 = amidino, amidrazono, oxazolidinyl, dialkylamino (including cyclic amines) R^3 = H, aryl (including hydroxyphenyl)
S2		R = alkyl R^1 = H, aryl R^2 = H, cyano, amidino, triazolyl
S3		R = aryl R^1 = phenyl, indolyl, amino, hydroxyl R^2 = cyano, sulfonyl R^3 = amino, cyano
S4		R = H, alkyl, aryl, R^1 = H, aryl R^2 = cyano, carbamoyl, cyanoformimidoyl, alkoxyformamidino R^3 = cyano, alkoxyalkylideneamine, amino, arylmethyleneamino, alkoxyformamidino
S5		R = alkyl R^1 = arylaminomethyleneamino, arylmethyleneamino, alkoxymethyleneamino
S6		R = alkyl R^1 = H, arylamino R^2 = H, methyl R^3 = aryl, amino, arylamino, alkyl (including hydroxyalkyl)
S7		R = alkyl, aryl (including hydroxyphenyl) R^1 = hydroxyphenyl
S8		R = aryl R^1 = H, acylamino, benzyloxy, hydroxyl R^2 = H, benzyloxy
S9		R = aryl R^1 = acylhydrazino
S10		R = aryl R^1 = alkyl (including hydroxyalkyl)
S11		R, R^1 = amino, arylaminomethyleneamino, arylmethyleneamino, alkoxyalkylideneamine, ureylene R^2 = cyano, carbamoyl

their chemotypes against all bioactive compounds for adenosine receptors present in the annotated chemical libraries used in this work confirmed the structural novelty of the hits. Figure 2 includes also further confirmation of the affinity and functional activity of the two compounds for their respective receptors. Concentration-

response binding competition curves (Fig. 2b) returned pK_i values of 7.8 ± 0.1 and 5.6 ± 0.1 at the A_1 and A_{2A} receptors for MSB-A1 and MSB-A2a, respectively, and measurements of the modulation of NECA-dependent intracellular cAMP formation by MSB-A1 and MSB-A2a (Fig. 2c) confirmed their antagonist behaviour with pK_b

Table 2
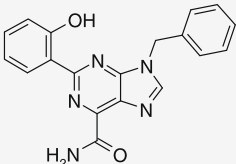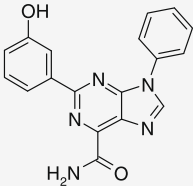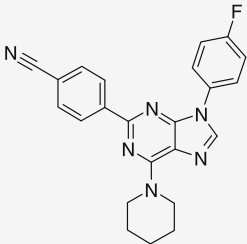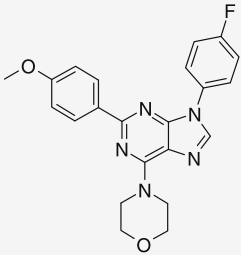In vitro screening of in silico-selected compounds on each adenosine receptor subtype
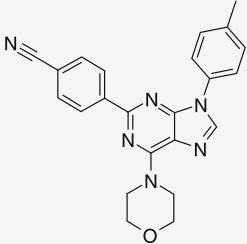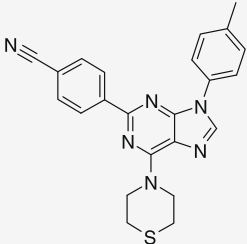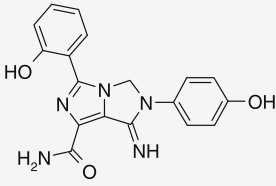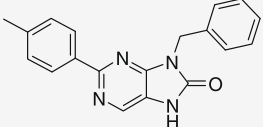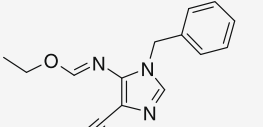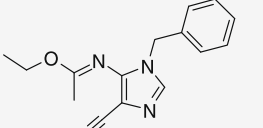
	A$_1$	A$_{2A}$	A$_{2B}$	A$_3$
1	11.1 ± 1.2	22.9 ± 4.7	9.5 ± 3.4	10.9 ± 0.8
2	25.5 ± 1.0	4.5 ± 1.8	0.5 ± 1.2	23.1 ± 0.5
3	0.8 ± 0.6	0.4 ± 1.1	6.9 ± 3.0	15.1 ± 3.8
4	18.8 ± 1.2	5.0 ± 0.7	3.0 ± 2.6	31.8 ± 2.7
5	7.6 ± 6.3	6.1 ± 1.4	6.8 ± 2.1	3.0 ± 1.2
6	6.8 ± 1.1	14.3 ± 3.1	4.3 ± 3.2	1.9 ± 0.6
7 MSB-A2b	26.8 ± 5.2	15.2 ± 2.7	**55.4 ± 2.5**	26.1 ± 2.5

Table 2 (continued)

	A$_1$	A$_{2A}$	A$_{2B}$	A$_3$
8	37.5 ± 2.1	20.0 ± 3.7	2.6 ± 1.7	**71.1 ± 1.3**
9	9.8 ± 3.0	15.2 ± 4.8	2.0 ± 1.1	1.9 ± 0.6
10	1.2 ± 0.3	9.8 ± 2.6	9.9 ± 4.2	28.0 ± 4.1

The 15 predictions made in silico are marked in light-grey. The two predictions with experimental values over 50% displacement of specific radioligand binding at 10 μM are highlighted in dark-grey.
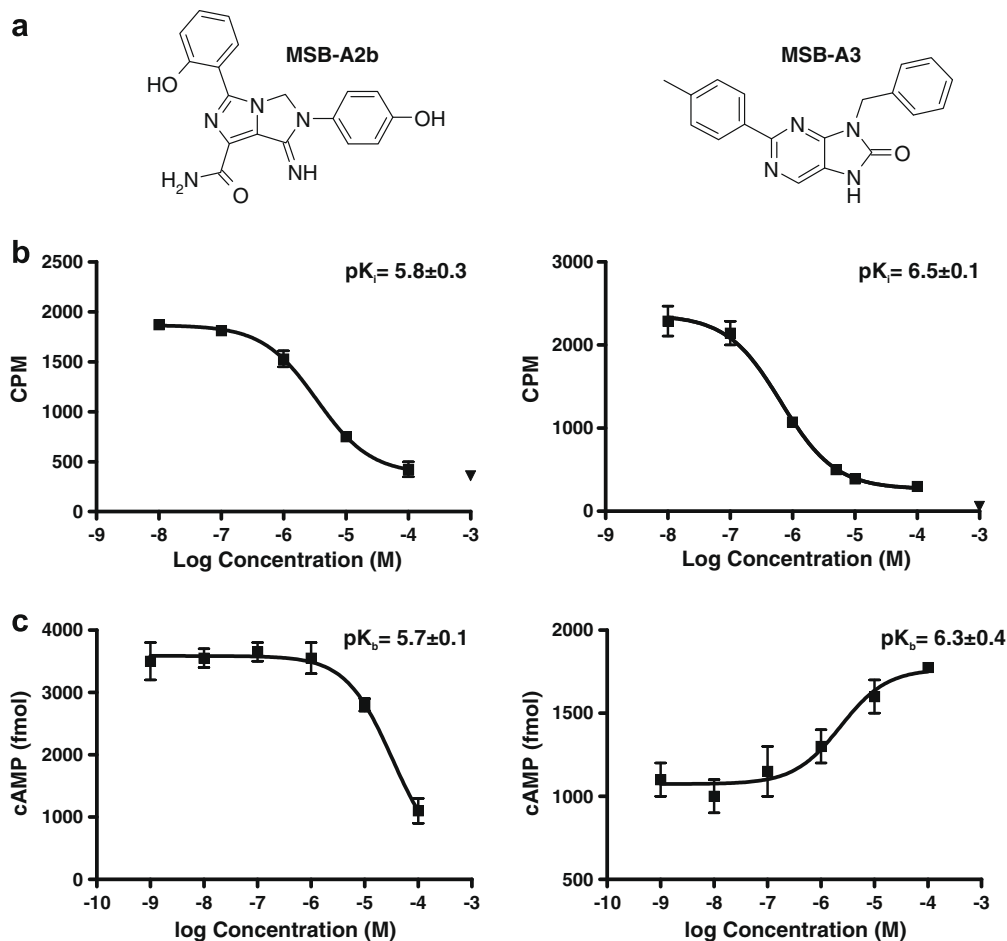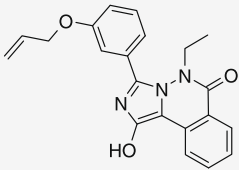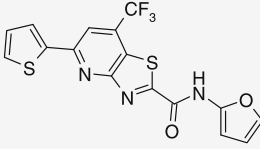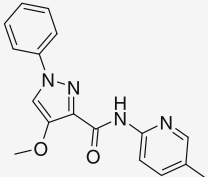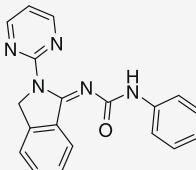

Figure 1. (a) Structures of the two hits for the (left) A$_{2B}$ and (right) A$_3$ receptors; (b) binding competition curves of (left) MSB-A2b (■) against 25 nM [³H]DPCPX at human A$_{2B}$ receptors, using 100 μM NECA for unmasking non-specific binding (▲) and (right) MSB-A3 (■) against 30 nM [³H]NECA at human A$_3$ receptors, using 100 μM R-PIA for unmasking non-specific binding (▲); and (c) modulation of cAMP formation of (left) MSB-A2b (■) over 10 μM NECA-induced cAMP accumulation at human A$_{2B}$ receptors and (right) MSB-A3 (■) over 10 μM NECA-induced cAMP decrease of 10 μM forskolin-stimulated human A$_3$ receptors. Points represent the mean ± S.E.M. (vertical bars) of two separate experiments.

Table 3
In vitro screening of the compounds purchased from commercial vendors on the A_1 and A_{2A} adenosine receptors

	Provider	A_1	A_{2A}
MSB-A1 11	Enamine	**87.3 ± 1.1**	10.9 ± 0.2
12	Enamine	**60.7 ± 3.9**	**70.5 ± 4.8**
13	Enamine	**51.9 ± 1.5**	**59.6 ± 6.7**
14	Enamine	38.5 ± 1.1	6.7 ± 4.7
MSB-A2a 15	ChemDiv	38.9 ± 11.7	**68.9 ± 2.5**
16	ChemDiv	8.0 ± 2.1	13.3 ± 1.2
17	Asinex	**79.0 ± 0.8**	**63.0 ± 2.3**
18	Pharmeks	18.8 ± 11.1	8.1 ± 6.7

The eight predictions with experimental values over 50% displacement of specific radioligand binding at 10 μM are highlighted in grey.

properties, all hits are found to be within the boundaries of the rule-of-five.[23] With respect to the binding profile, all antagonists were found to be reasonably selective for their corresponding adenosine receptors. Only MSB-A2a showed similar affinity values for the A_{2A} and A_3 receptors. Considering the fact that no optimisation activities on the binding and selectivity of the four antagonists took place, this is a remarkable outcome. In addition, little is known in the literature about the polypharmacology of adenosine receptor antagonists.[21] To further assess the degree of selectivity of those hits beyond its own protein family, they were tested in primary screens against three diverse amine GPCRs, namely, the adrenergic α_{2A}, the histamine H_1, and the serotonin 5-HT$_7$ receptors. The results show that the percentage of displacement of radioligand binding at 10 μM for those amine GPCRs is in all cases below 50%. In fact, only for the interaction between antagonists MSB-A1 and MSB-A2a and the H1 receptor values close to 40% are obtained, whereas all other interactions show values below 30%.

3. Conclusions

In silico target profiling methods are emerging as efficient alternatives to the currently unaffordable high-throughput in vitro target profiling of millions of compounds over hundreds of biological targets. All these methods capitalize on the vast amount of prior knowledge on bioactive ligands and protein structures available for many targets of therapeutic relevance,[12] having led recently to the successful identification of novel targets for known drugs.[17] As both pharmacological and structural data on ligand–target interactions are becoming increasingly available, it is expected that the performance of these knowledge-based methods will improve significantly reaching enough maturity to be able to not only identify novel targets but to characterize the entire pharmacological profile of compounds. In addition, exploration of the biological space for molecules has been traditionally focussed on commercially available compounds and target-directed libraries from internal corporate projects, which represent just a minute portion of the potentially synthetically accessible chemical space. However, large numbers of synthesis-driven compounds, often covering novel areas of chemical space, are sitting on the shelves of academic chemistry laboratories without ever being considered for biological screening. In this respect, the development of novel in silico methods for target profiling might help directing the biological space relevant for each chemical collection and thus promoting and strengthening collaborative efforts between chemists and biologists.[24] A good example has been presented here, leading to the identification of novel antagonists covering all members of the adenosine receptor family. This is, to the best of our knowledge, the first time that in silico directed chemical probing of an entire protein family has been attempted and successfully achieved.

4. Materials and methods

4.1. In silico target profiling

Our in silico target profiling approach relies on the assumption that the set of bioactive ligands collected for a given target provides a complementary description of the target from a ligand perspective. In order to be able to process this information efficiently, molecular structures need to be encoded using some sort of mathematical descriptors. In this respect, a novel set of low-dimension molecular descriptors called SHED were used.[22] SHED are derived from distributions of atom-centered feature pairs extracted directly from the topology of molecules. The collection of SHED values reflecting the overall distribution of pharmacophoric features in a molecule constitutes its SHED profile. The ensemble of

values of 6.8 ± 0.2 and 5.1 ± 0.3 at the A_1 and A_{2A} receptors, respectively.

Finally, the property and binding profiles of the four antagonists identified are summarized in Table 4. In terms of molecular

F. M. Areias et al./Bioorg. Med. Chem. 18 (2010) 3043–3052

3049

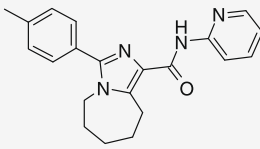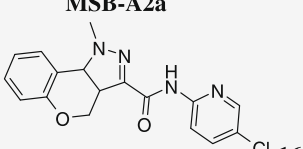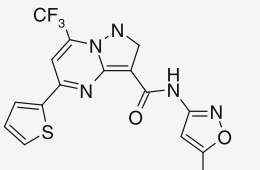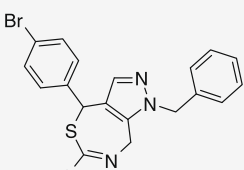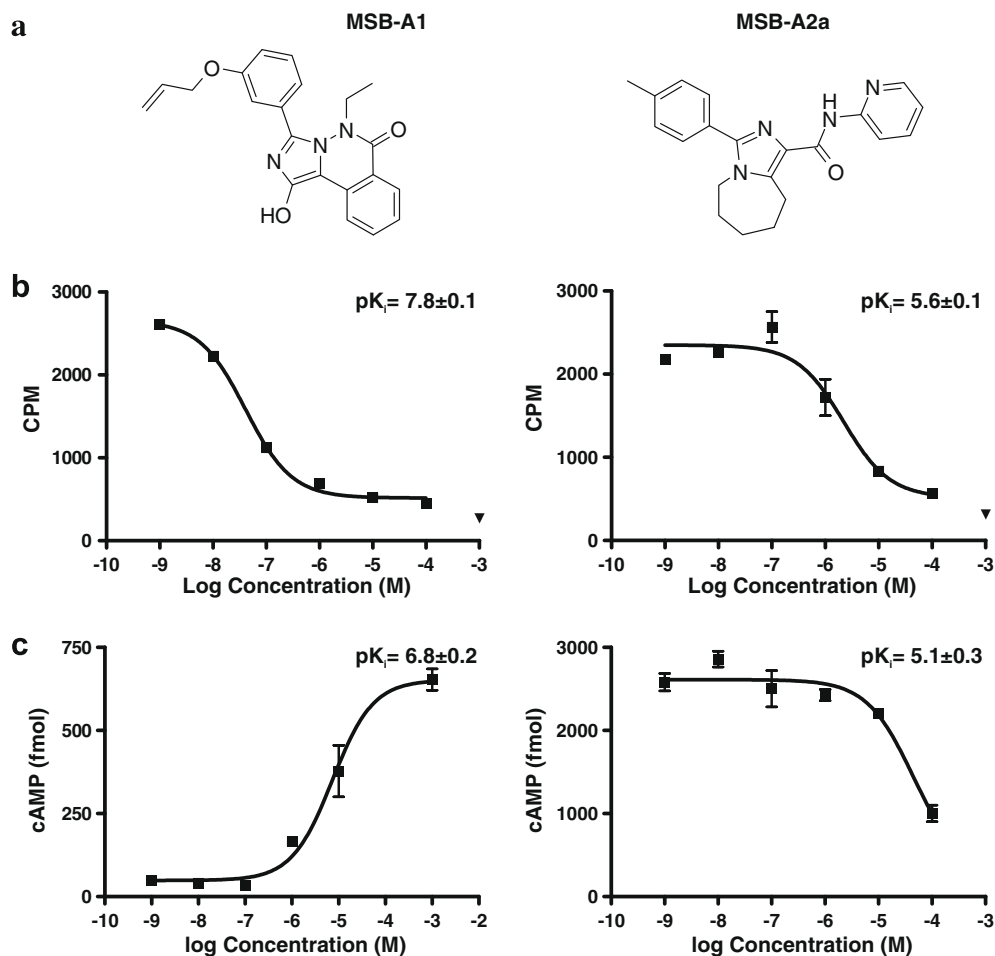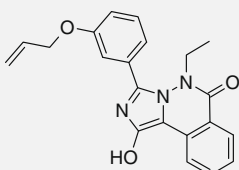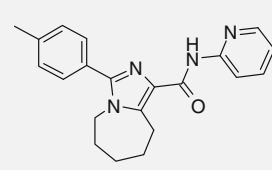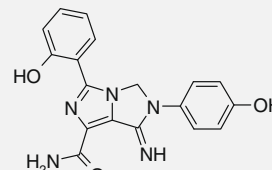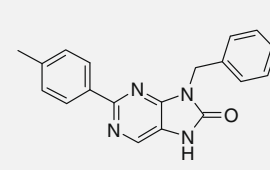**Figure 2.** (a) Structures of the two hits for the (left) A_1 and (right) A_{2A} receptors; (b) binding competition curves of (left) MSB-A1 (■) against 1.4 nM [³H]DPCPX at human A_1 receptors, using 10 μM R-PIA for unmasking non-specific binding (▲) and (right) MSB-A2a (■) against 3 nM [³H]ZM241385 at human A_{2A} receptors, using 50 μM NECA for unmasking non-specific binding (▲); and (c) modulation of cAMP formation of (left) MSB-A1 (■) over 0.1 μM NECA-induced cAMP decrease of 10 μM forskolin-stimulated human A_1 receptors and (right) MSB-A2a (■) over 1 μM NECA-induced cAMP accumulation at human A_{2A} receptors. Points represent the mean ± S.E.M. (vertical bars) of two separate experiments.

Table 4
Property and binding profiles of the novel antagonists identified for each one of the four adenosine receptors

	MSB-A1	MSB-A2a	MSB-A2b	MSB-A3
Property profile				
MW	361.4	346.4	350.4	316.4
clogP	4.58	4.45	1.58	4.44
HBA	3	3	4	3
HBD	1	1	4	1
Binding profile				
A_1	**7.8 ± 0.1**	39%	27%	38%
A_{2A}	11%	**5.6 ± 0.1**	15%	20%
A_{2B}	5%	19%	**5.8 ± 0.3**	3%
A_3	39%	**5.5 ± 0.2**	26%	**6.5 ± 0.1**
α_{2A}	14%	12%	28%	18%
H_1	42%	39%	17%	17%
$5\text{-}HT_7$	20%	18%	11%	1%

SHED profiles representing all bioactive molecules annotated to a particular protein target forms a mathematical description of the target from a chemical perspective. On this basis, ligand-based descriptor models were derived for 86 GPCRs using the interaction data present in BindingDB[9] and PDSP,[25] supplemented with an additional GPCR annotated chemical library assembled internally. The probability of any molecule to interact with a particular target is assumed to be related to the degree of similarity relative to the set of known bioactive ligands for that target. Accordingly, Euclidean distances between the SHED profile of a molecule and all SHED profiles associated to a target are first calculated and a final target scoring is given by the minimum value of all Euclidean distances. Following a previous validation analysis,[26] if that minimum Euclidean distance is below 0.6, the molecule receives an annotation to the target.

4.2. Chemical synthesis and characterization

4.2.1. Compound MSB-A1

5-Ethyl-1-hydroxy-3-(3-(vinyloxy)phenyl)imidazo[5,1-a]phthalazin-6(5H)-one was purchased from Enamine Ltd with guaranteed purity of 96%.

4.2.2. Compound MSB-A2a

6,7,8,9-Tetrahydro-N-(pyridin-2-yl)-3-p-tolyl-5H-imidazo[1,5-a]azepine-1-carboxamide was purchased from ChemDiv Inc. with guaranteed purity of 95%.

4.2.3. Compound MSB-A2b

(1-Carbamoyl-7-imino-6,7-dihydro-3-(2′-hydroxyphenyl)-6-(4″-hydroxyphenyl)-imidazo[1,5-e]imidazole) was synthesized using the following experimental procedure: Triethylamine (0.37 mL, 2.74 mmol) was added to a solution of N^1-(2-amino-1,2-dicyanovinyl)-N^2-(4′-hydroxyphenyl)formamidine (0.10 g, 0.44 mmol) and 2-hydroxybenzaldehyde (0.05 mL, 0.47 mmol) in ethyl acetate (3 mL) and ethanol (0.3 mL). The mixture was stirred at 0 to 4 °C, under a nitrogen atmosphere, until the starting material was totally consumed (17 days). The cream solid suspension was filtered and washed with ethyl acetate and diethyl ether. The solid was recrystallized from acetone, leading to an analytically pure sample of the product (0.05 g, 0.15 mmol, 34%). Spectroscopic characterization of MSB-A2b yielded the following: ^{1}H NMR (300 MHz, DMSO-d_6): δ 11.38 (s, 1H), 9.33 (s, 1H), 9.08 (s, 1H), 8.27 (s, 1H), 7.82 (d, 2H, J = 8.4 Hz), 7.69 (d, 1H, J = 6.9 Hz), 7.63 (s, 1H), 7.39 (t, 1H, J = 7.2 Hz), 7.04 (d, 1H, J = 8.1 Hz), 6.93–7.00 (m, 1H), 6.80 (d, 2H, J = 8.4 Hz), 6.18 (s, 2H). ^{13}C NMR (75 MHz, DMSO-d_6): δ 64.74, 112.50, 115.22, 117.14, 119.38, 120.62, 126.94, 128.82, 131.17, 131.40, 132.86, 139.87, 150.72, 153.34, 156.35, 163.46. HRMS (m/z): calcd $C_{18}H_{15}N_5O_3$ requires MH$^+$, 350.1208; found MH$^+$, 350.1249.

N^1-(2-Amino-1,2-dicyanovinyl)-N^2-(4′-hydroxyphenyl)formamidine, used as starting material, was obtained from the reaction of ethyl-N-(2-amino-1,2-dicyanovinyl)formimidate and 2-hydroxyaniline, using a synthetic method previously described for the preparation of analogous compounds.[27]

4.2.4. Compound MSB-A3

(9-Benzyl-2-(4-methylphenyl)-7,9-dihydro-8H-purin-8-one) was synthesized through the following method: piperidine (0.03 g, 0.35 mmol) was added to a solution of 2-(1-benzyl-5-imino-2-oxo-imidazolidin-4-ylidene)-3-(phenylmethyleneamino)propanenitrile (0.12 g, 0.35 mmol) in ethanol (20 mL) and the mixture was stirred at room temperature for 5 days. The solvent was partially removed in the rotary evaporator leading to a white solid. The product was filtered, washed with diethyl ether and ethanol and identified as the title compound (0.10 g, 0.32 mmol, 91%). Spectroscopic

characterization of MSB-A3 yielded the following: ^{1}H NMR (300 MHz, DMSO-d_6): δ 11.48 (broad s, 1H), 8.31 (s, 1H), 8.20 (d, 2H, J = 8.2 Hz), 7.40 (d, 2H, J = 7.2 Hz), 7.32 (t, 2H, J = 8.0 Hz), 7.26 (brd, 2H, J = 8.2 Hz), 5.05 (s, 2H), 2.33 (s, 3H). ^{13}C NMR (75 MHz, DMSO-d_6): δ 21.01, 42.58, 120.48, 127.13, 127.71, 127.85, 128.71, 129.24, 133.28, 134.99, 136.70, 139.54, 150.34, 153.36, 156.23. Anal. Calcd $C_{19}H_{16}N_4O·0.2H_2O$ requires: C, 71.32; H, 5.17; N, 17.51. Found: C, 71.20; H, 5.38; N, 17.57.

9-Benzyl-2-(4-methylphenyl)-7,9-dihydro-8H-purin-8-one, used as starting material, was obtained from the reaction of diaminomaleonitrile with benzylisocyanate, followed by addition of 4-tolualdehyde and DBU, in three consecutive steps.[28]

4.3. Radioligand binding assays

Compounds were assayed at the concentration of 10 μM at all receptors following the conditions stated above. Concentration-response binding competition curves at all adenosine receptors were carried out by assaying six different concentrations (range between 10 nm to 100 μM) of the compounds MSB-A1, MSB-A2a, MSB-A2b and MSB-A3. The −log of inhibition constant (pK_i) of each compound was calculated by the Cheng–Prusoff equation, $K_i = IC_{50}/(1 + [L]/K_D)$, where IC_{50} is the concentracion of compound that displaces the binding of radioligand by 50%, $[L]$ is the free concentration of radioligand and K_D is the dissociation constant of each radioligand. IC_{50} values were obtained by fitting the data with non-linear regression, with Prism 2.1 software (GraphPad, San Diego, CA).

4.3.1. Human A_1 receptors

Adenosine A_1 receptor competition binding experiments were carried out in membranes from CHO-A_1 cells (Euroscreen, Gosselies, Belgium). On the day of assay, membranes were defrosted and re-suspended in incubation buffer 20 mM Hepes, 100 mM NaCl, 10 mM $MgCl_2$, 2 units/ml adenosine deaminase (pH 7.4). Each reaction well of a GF/C multiscreen plate (Millipore, Madrid, Spain), prepared in duplicate, contained 15 μg of protein, 2 nM [^{3}H]DPCPX and test compound. Non-specific binding was determined in the presence of 10 μM (R)-PIA. The reaction mixture was incubated at 25 °C for 60 min, after which samples were filtered and measured in a microplate beta scintillation counter (Microbeta Trilux, Perkin Elmer, Madrid, Spain).

4.3.2. Human A_{2A} receptors

Adenosine A_{2A} receptor competition binding experiments were carried out in membranes from HeLa-A_{2A} cells. On the day of assay, membranes were defrosted and re-suspended in incubation buffer 50 mM Tris–HCl, 1 mM EDTA, 10 mM $MgCl_2$ and 2 UI/mL adenosine deaminase (pH 7.4). Each reaction well of a GF/C multiscreen plate (Millipore, Madrid, Spain), prepared in duplicate, contained 10 μg of protein, 3 nM [^{3}H]ZM241385 and test compound C0036E08. Non-specific binding was determined in the presence of 50 μM NECA. The reaction mixture was incubated at 25 °C for 30 min, after which samples were filtered and measured in a microplate beta scintillation counter (Microbeta Trilux, Perkin Elmer, Madrid, Spain).

4.3.3. Human A_{2B} receptors

Adenosine A_{2B} receptor competition binding experiments were carried out in membranes from HEK-293-A_{2B} cells (Euroscreen, Gosselies, Belgium) prepared following the provider's protocol. On the day of assay, membranes were defrosted and re-suspended in incubation buffer 50 mM Tris–HCl, 1 mM EDTA, 10 mM $MgCl_2$, 0.1 mM benzamidine, 10 μg/ml bacitracine and 2 UI/mL adenosine deaminase (pH 6.5). Each reaction well prepared in duplicate, contained 18 μg of protein, 35 nM [^{3}H]DPCPX and test compound.

Non-specific binding was determined in the presence of 400 μM NECA. The reaction mixture was incubated at 25 °C for 30 min, after which samples were filtered through a multiscreen GF/C microplate and measured in a microplate beta scintillation counter (Microbeta Trilux, Perkin Elmer, Madrid, Spain).

4.3.4. Human A$_3$ receptors

Adenosine A$_3$ receptor competition binding experiments were carried out in membranes from HeLa-A$_3$ cells. On the day of assay, membranes were defrosted and re-suspended in incubation buffer 50 mM Tris–HCl, 1 mM EDTA, 5 mM MgCl$_2$ and 2 UI/mL adenosine deaminase (pH 7.4). Each reaction well of a GF/B multiscreen plate (Millipore, Madrid, Spain), prepared in triplicate, contained 90 μg of protein, 30 nM [^{3}H]NECA and test compound. Non-specific binding was determined in the presence of 100 μM (R)-PIA. The reaction mixture was incubated at 25 °C for 180 min, after which samples were filtered and measured in a microplate beta scintillation counter (Microbeta Trilux, Perkin Elmer, Madrid, Spain).

4.3.5. Human α$_{2A}$ receptors

Adrenergic α$_{2A}$ receptor competition binding experiments were carried out in membranes from CHO-α$_{2A}$ cells. On the day of assay, membranes were defrosted and re-suspended in incubation buffer 25 mM Na$_2$PO$_4$ (pH 7.4). Each reaction well of a GF/C multiscreen plate (Millipore, Madrid, Spain), prepared in duplicate, contained 25 μg of protein, 0.37 nM [^{3}H]MK-912 and test compound. Non-specific binding was determined in the presence of 100 μM norepinephrine. The reaction mixture was incubated at 25 °C for 30 min, after which samples were filtered and measured in a microplate beta scintillation counter (Microbeta Trilux, Perkin Elmer, Madrid, Spain).

4.3.6. Human H$_1$ receptors

Histamine H$_1$ receptor competition binding experiments were carried out in membranes from CHO-H$_1$ cells. On the day of assay, membranes were defrosted and re-suspended in incubation buffer 50 mM Tris–HCl (pH 7.4). Each tube prepared in duplicate, contained 1 μg of protein, 2 nM [^{3}H]pyrilamine and test compound. Non-specific binding was determined in the presence of 10 μM triprolidine. The reaction mixture was incubated at 27 °C for 60 min, after which samples were filtered through GF/C filters using a Brandel Harvester and measured in a beta scintillation counter (Beckman LS600 LL, Beckman Coulter, Madrid, Spain).

4.3.7. Human 5-HT$_7$ receptors

Serotonin 5-HT$_7$ receptor competition binding experiments were carried out in membranes from HEK-293-5-HT$_7$ cells. On the day of assay, membranes were defrosted and re-suspended in incubation buffer 50 mM Tris–HCl, 4 mM CaCl$_2$, 1 mM ascorbic acid, 0.1 mM pargyline (pH 7.4). Each reaction well of a GF/C multiscreen plate (Millipore, Madrid, Spain), prepared in duplicate, contained 5 μg of protein, 2 nM [^{3}H]SB269970 and test compound. Non-specific binding was determined in the presence of 25 μM clozapine. The reaction mixture was incubated at 37 °C for 60 min, after which samples were filtered and measured in a microplate beta scintillation counter (Microbeta Trilux, Perkin Elmer, Madrid, Spain).

4.4. cAMP prodution measurement

These assays were performed at adenosine receptors transfected using a cAMP enzyme-immunoassay kit (Amersham Biosciences) and competition curves were obtained for compounds MSB-A1, MSB-A2a, MSB-A2b and MSB-A3. Since A$_{2A}$ and A$_{2B}$ receptors are Gs-coupled receptors competition curves where performed over the NECA-induced cAMP accumulation. By other side, A$_1$ and

A$_3$ receptors are Gi/o-coupled receptors and therefore competition curves were performed over the NECA-induced inhibition of forskolin-induced cAMP accumulation.

The antagonist potency was expressed as pK_B ($-$log of the dissociation constant, K_B), calculated for one concentration of antagonist following the equation proposed by Leff and Dougall, $K_B = IC_{50}/((2 + ([A]/[A_{50}])^n)^{1/n} - 1)$, where IC_{50} is the concentration of antagonist that inhibits receptor activation in a 50%, [A] is the agonist concentration used to stimulate the receptor under study, [A$_{50}$] is the concentration of agonist that elicits a half-maximal stimulation of the receptor and n is the slope of the antagonist concentration-response curve.

4.4.1. Human A$_1$ receptors

CHO-A$_1$ cells were seeded (20,000 cells/well) in 96-well culture plates and incubated at 37 °C in an atmosphere with 5% CO$_2$ in Eagle's Medium Nutrient Mixture F-12 (EMEM F-12), containing 10% Foetal Calf Serum (FCS) and 1% L-Glutamine. Cells were washed 3× with 200 μl assay medium (EMEM-F12 and 25 mM HEPES pH 7.4) and pre-incubated with assay medium containing 20 μM rolipram and test compounds at 37 °C for 15 min. 0.1 μM NECA was incubated for 15 min at 37 °C and 3 μM forskolin was incubated for 3 min (total incubation time 30 min). Reaction was stopped with lysis buffer supplied in the kit and the enzyme-immunoassay was carried out for detection of intracellular cAMP at 450 nm in an Ultra Evolution detector (Tecan). Data were fitted by non-linear regression using GraphPad Prism v2.01 (GraphPad Software).

4.4.2. Human A$_{2A}$ receptors

CHO-A$_{2A}$ cells were seeded (10,000 cells/well) in 96-well culture plates and incubated at 37 °C in an atmosphere with 5% CO$_2$ in Dulbecco's Modified Eagle's Medium Nutrient Mixture F-12 (DMEM F-12), containing 10% Foetal Calf Serum (FCS) and 1% L-Glutamine. Cells were washed 3× with 200 μl assay medium (DMEM-F12 and 25 mM HEPES pH 7.4) and pre-incubated with assay medium containing 30 μM rolipram and test compounds at 37 °C for 15 min. 1 μM NECA was incubated for 15 min at 37 °C (total incubation time 30 min). Reaction was stopped with lysis buffer supplied in the kit and the enzyme-immunoassay was carried out for detection of intracellular cAMP at 450 nm in an Ultra Evolution detector (Tecan). Data were fitted by non-linear regression using GraphPad Prism v2.01 (GraphPad Software).

4.4.3. Human A$_{2B}$ receptors

HEK-293 cells were seeded (10,000 cells/well) in 96-well culture plates and incubated at 37 °C in an atmosphere with 5% CO$_2$ in Eagle's Medium Nutrient Mixture F-12 (EMEM F-12), containing 10% Foetal Calf Serum (FCS) and 1% L-Glutamine. Cells were washed 3× with 200 μl assay medium (EMEM-F12 and 25 mM HEPES pH 7.4) and pre-incubated with assay medium containing 30 μM rolipram and test compounds at 37 °C for 15 min. 10 μM NECA was incubated for 15 min at 37 °C (total incubation time 30 min). Reaction was stopped with lysis buffer supplied in the kit and the enzyme-immunoassay was carried out for detection of intracellular cAMP at 450 nm in an Ultra Evolution detector (Tecan). Data were fitted by non-linear regression using GraphPad Prism v2.01 (GraphPad Software).

4.4.4. Human A$_3$ receptors

CHO-A$_3$ cells were seeded (20,000 cells/well) in 96-well culture plates and incubated at 37 °C in an atmosphere with 5% CO$_2$ Dulbecco's Modified Eagle's Medium Nutrient Mixture F-12 (DMEM F-12), containing 10% Foetal Calf Serum (FCS) and 1% L-Glutamine. Cells were washed 3x with 200 μl assay medium (DMEM-F12 and 25 mM HEPES pH 7.4) and pre-incubated with assay medium containing 30 μM rolipram and test compounds at 37 °C for 15 min.

1 µM NECA was incubated for 15 min at 37 °C and 10 µM forskolin was incubated for 3 min (total incubation time 30 min). Reaction was stopped with lysis buffer supplied in the kit and the enzyme-immunoassay was carried out for detection of intracellular cAMP at 450 nm in an Ultra Evolution detector (Tecan). Data were fitted by non-linear regression using GraphPad Prism v2.01 (GraphPad Software).

Acknowledgements

Supplementary data

Supplementary data (full list of the 86 G protein-coupled receptors against which in silico target profiling was performed, together with the predicted number of annotations assigned to each target) associated with this article can be found, in the online version, at doi:10.1016/j.bmc.2010.03.048.

References and notes

1. Schreiber, S. L. *Nat. Chem. Biol.* **2005**, *1*, 64.
2. Krejsa, C. M.; Horvath, D.; Rogalski, S. L.; Penzotti, J. E.; Mao, B.; Barbosa, F.; Migeon, J. C. *Curr. Opin. Drug Discov. Devel.* **2003**, *6*, 470.
3. Whitebread, S.; Hamon, J.; Bojanic, D.; Urban, L. *Drug Discovery Today* **2005**, *10*, 1421.
4. Karaman, M. W.; Herrgard, S.; Treiber, D. K.; Gallant, P.; Atteridge, C. E.; Campbell, B. T.; Chan, K. W.; Ciceri, P.; Davis, M. I.; Edeen, P. T.; Faraoni, R.; Floyd, M.; Hunt, J. P.; Lockhart, D. J.; Milanov, Z. V.; Morrison, M. J.; Pallares, G.; Patel, H. K.; Pritchard, S.; Wodicka, L. M.; Zarrinkar, P. P. *Nat. Biotechnol.* **2008**, *26*, 127.
5. Austin, C. P.; Brady, L. S.; Collins, F. S. *Science* **2004**, *306*, 1138.
6. Jensen, N. H.; Roth, B. L. *Comb. Chem. High Throuput Screening* **2008**, *11*, 420.
7. Wishart, D. S.; Knox, C.; Guo, A. C.; Cheng, D.; Shrivastava, S.; Tzur, D.; Gautam, B.; Hassanali, M. *Nucleic Acids Res.* **2008**, *36*, D901.
8. Harmar, A. J.; Hills, R. A.; Rosser, E. M.; Jones, M.; Buneman, O. P.; Dunbar, D. R.; Greenhill, S. D.; Hale, V. A.; Sharman, J. L.; Bonner, T. I.; Catterall, W. A.; Davenport, A. P.; Delagrange, P.; Dollery, C. T.; Foord, S. M.; Gutman, G. A.; Laudet, V.; Neubig, R. R.; Ohlstein, E. H.; Olsen, R. W.; Peters, J.; Pin, J. P.; Ruffolo, R. R.; Searls, D. B.; Wright, M. W.; Spedding, M. *Nucleic Acids Res.* **2009**, *37*, D680.
9. Liu, T.; Lin, Y.; Wen, X.; Jorissen, R. N.; Gilson, M. K. *Nucleic Acids Res.* **2007**, *35*, D198.
10. Berman, H. M.; Westbrook, J.; Feng, Z.; Gilliland, G.; Bhat, T. N.; Weissig, H.; Shindyalov, I. N.; Bourne, P. E. *Nucleic Acids Res.* **2000**, *28*, 235.
11. Jenkins, J. L.; Bender, A.; Davies, J. W. *Drug Discovery Today: Technol.* **2006**, *3*, 413.
12. Ekins, S.; Mestres, J.; Testa, B. *Br. J. Pharmacol.* **2007**, *152*, 9.
13. Jenwitheesuk, E.; Horst, J. A.; Rivas, K. L.; van Voorhis, W. C.; Samudrala, R. *Trends Pharmacol. Sci.* **2008**, *29*, 62.
14. Keiser, M. J.; Roth, B. L.; Armbruster, B. N.; Ernsberger, P.; Irwin, J. J.; Shoichet, B. K. *Nat. Biotechnol.* **2007**, *25*, 197.
15. Plouffe, D.; Brinker, A.; McNamara, C.; Henson, K.; Kato, N.; Kuhen, K.; Nagle, A.; Adrián, F.; Matzen, J. T.; Anderson, P.; Nam, T. G.; Gray, N. S.; Chatterjee, A.; Janes, J.; Yan, S. F.; Trager, R.; Caldwell, J. S.; Schultz, P. G.; Zhou, Y.; Winzeler, E. A. *Proc. Natl. Acad. Sci. U.S.A.* **2008**, *105*, 9059.
16. Muller, P.; Lena, G.; Boilard, E.; Bezzine, S.; Lambeau, G.; Guichard, G.; Rognan, D. J. *Med. Chem.* **2006**, *49*, 6768.
17. Rollinger, J. M.; Schuster, D.; Danzl, B.; Schwaiger, S.; Markt, P.; Schmidtke, M.; Gertsch, J.; Raduner, S.; Wolber, G.; Langer, T.; Stuppner, H. *Planta Med.* **2009**, *75*, 195.
18. Gregori-Puigjané, E.; Mestres, J. *Comb. Chem. High Throughput Screening* **2008**, *11*, 669.
19. Jacobson, K. A.; Gao, Z. G. *Nat. Rev. Drug Disc.* **2006**, *5*, 247.
20. Haskó, G.; Linden, J.; Cronstein, B.; Pacher, P. *Nat. Rev. Drug Disc.* **2008**, *7*, 759.
21. Baraldi, P. G.; Tabrizi, M. A.; Gessi, S.; Borea, P. A. *Chem. Rev.* **2008**, *108*, 238.
22. Gregori-Puigjané, E.; Mestres, J. *J. Chem. Inf. Model.* **2006**, *46*, 1615.
23. Lipinski, C. A. *Drug Discovery Today: Technol.* **2004**, *1*, 337.
24. Muir, T. W. *ACS Chem. Biol.* **2009**, *4*, 241.
25. Roth, B. L.; Lopez, E.; Beischel, S.; Westkaemper, R. B.; Evans, J. M. *Pharmacol. Ther.* **2004**, *102*, 99.
26. Mestres, J.; Martin-Couce, L.; Gregori-Puigjané, E.; Cases, M.; Boyer, S. *J. Chem. Inf. Model.* **2006**, *46*, 2725.
27. Booth, B. L.; Dias, A. M.; Proença, M. F. *J. Chem. Soc., Perkin Trans. I* **1992**, 2119.
28. Booth, B. L.; Dias, A. M.; Proença, M. F.; Zaki, M. E. A. *J. Org. Chem.* **2001**, *66*, 8436.